Design proposal for high-efficiency, high-power density dual interleaved LLC converter with interactive control interface

PAVOL SPANIK, MICHAL FRIVALDSKY, ONDREJ HOCK, ANDREJ KANOVSKY
Department of mechatronics and electronics
University of Zilina
Univerzitna 1, 010 26, Zilina
SLOVAKIA
michal.frivaldsky@fel.uniza.sk

Abstract: - Dual interleaved LLC resonant converter with half bridge topology of main circuit characterized by high switching frequency, high power density and high efficiency over entire operational range is initially described. Consequently, the proposal for a computer control is given. Given type of control approach has been developed for the laboratory testing of resonant converters. The control system is implemented within DSP. The communication between control system and user is implemented by a control panel running on host computer (i.e. PC).

Key-Words: - power density, interleaved LLC, computer control system, Launchpad TMS320F2802x, high efficiency, experimental testing

1 Introduction

Energy efficiency and power density become main qualitative indexes of power electronic systems. Key factors for continual increase of both indicators have environmental, as well as economical character. LLC resonant converters have been discovered already in the seventies of the twentieth century, but the mass of the deployment occurs only in recent years because of their unique properties, and high efficiency [1-4].

Operation at high switching frequency, soft commutation of power switches, optimal selection of power switches, the selection of magnetic core are prerequisites for the successful design of the high power density supply. It should also be noted, that the use of higher switching frequencies however brings also some negatives. One of such negative impacts of high switching frequency operation is linear increase of switching losses of semiconductor devices, which consequently will negatively affect the efficiency of the entire power system [5]-[8].

This article describes design of dual interleaved, parallel – operated LLC resonant converters for application, where very high efficiency in wide load range, together with high power density, with output power greater than 1 kW is required. Also the possibility of computer control of perspective resonant converters is being described. Proposed control strategy enables in simple way to discover each operational characteristic of any power resonant converter. The proposal is verified on the dual-interleaved LLC converter.

2 Concept of the high efficiency, wide-load operated high power density power supply

An application area of the LLC half-bridge DC/DC converter is in the power range from tens of watts up to one kilowatt [9], [10]. Full bridge topology is preferable, when output power in the range of 10 kW is required

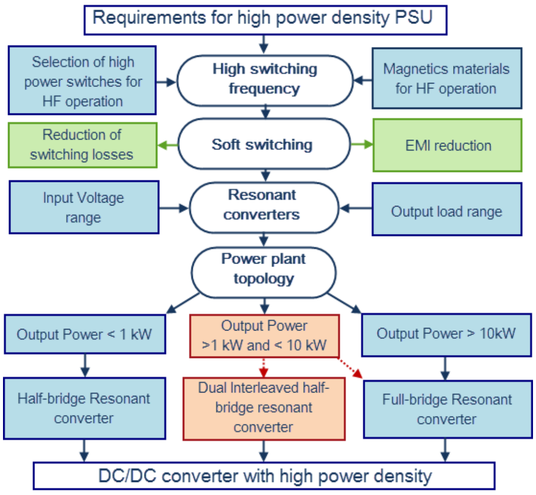

Fig. 1. Simplified design procedure for high power density DC/DC converter

At this point the question arises.

- What is the appropriate topology for power supplies with high power density and with output power over 1kW?
- Is it possible to use half-bridge topology?
- Or is it better to take advantage of the full bridge?

Answers to these questions are not clear and are subjected to the requirements of the target. Advantages of the parallel operation of the LLC converters are highly appreciated in the applications where high efficiency is required for wide range of the output load. Telecommunications are the typical example due to variation of the load depends on the day/night traffic.

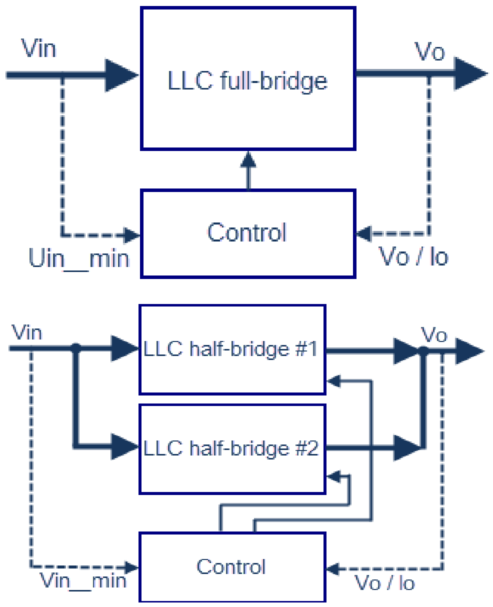

Fig. 2. Block schematic of full-bridge LLC converter (left) and dual half-bridge LLC converter (right)

Based on the performed investigation it seems that for applications with output power of 1 kW and low output voltage is more convenient to use the involvement of two parallel-operated LLC converters. The main reason is great advantage of this solution in the possibility of parallel operation of two DC / DC converters during heavy load and disconnection of one of the converter during light load. This unique feature involving two parallel - operated LLC converters has a favorable effect on achieving the higher efficiencies at low load (disconnecting one of the converters). Also due to the current cancellation effect (interleaved mode with 90 degrees of phase shift) a significant drop of output current ripple during heavy load can be achieved. Mentioned reduction is also beneficial for increase of the lifetime of the output capacitors.

In next chapters, more detailed description about the high-efficiency/high power density oriented design of dual interleaved, parallel – operated LLC converter will be given. We have focused on proper design of the most critical circuit component – transformer and output capacitor. Target input-output parameters of proposed converter are:

- Input voltage range 340Vdc – 400Vdc
- Maximal output power 2.4 kW
- Nominal output voltage 48Vdc
- Switching frequency: 500 kHz

2.1 High-frequency transformer design constrains for proposed converter type

More than ten years ago, a typical value for power density of proposed converters was around 0,304W/cm3 (5W/inch3). Nowadays its value for the same device is targeting values around 1,5W/cm3 (25W/inch3) [11] - [15]. There are several ways, how to meet upcoming requirements investigation of gain characteristic of power converter. In this part, the influence of proper material selection, as well as geometry of transformer core will be described.

Optimization of transformer design for high efficiency and high power density converter is subjected to the reduction of overall transformer losses. These losses are composed from losses in windings and losses in transformer core (hysteresis losses, eddy currents). As will be later shown, both components of transformer losses are affected by maximal value of magnetic induction, so the proper choice of this parameter is crucial.

For copper losses, next formula can be derived:

$$P_{Cu} = I_{tot}^2 R_{Cu} = \frac{I_{tot}^2 n_1^2 (MLT)\rho}{S_O K_U} \tag{1}$$

$$I_{tot} = \sum_{j=1}^{k} \frac{n_j}{n_1} I_j \tag{2}$$

where

I_{2tot} –RMS value of winding currents [A]
R_{Cu}–resistance of conductor in winding [Ω]
ρ –Wire effective resistivity [Ωm]
l_j–length of the conductor [cm]
n_1–number of turns – primary winding
(MLT) –Mean Length per Turn [cm]
S_O–surface utilization factor [cm2]

$$\Delta B = 10^4 \frac{\int_{t1}^{t2} u_1(t)dt}{2n_1 S_j} = 10^4 \frac{U_1}{2n_1 S_j} \tag{3}$$

where

$u_1(t)$–value of voltage on given winding [V/µs]

S_j–area of core [cm2]

From equation (3) the number of turns for requested value of magnetic induction has this formulation:

$$n_1 = 10^4 \frac{U_1}{2\Delta B S_j} \tag{4}$$

Substituting (4) and (2) into (1) yields to required dependency of losses in transformer windings on induction ripple ΔB:

$$P_{cu} = \left(\frac{\rho\, \lambda_1^2 I_{tot}^2}{4\, K_u}\right) \cdot \left(\frac{(MLT)}{W_A A_C^2}\right) \cdot \left(\frac{1}{\Delta B}\right)^2 \tag{5}$$

where $\lambda_1 = U_{in\_max} \cdot T_{sw} \cdot D$

From above mentioned equations is clear, that within increase of ripple content in magnetic induction, the losses in transformer windings will decrease rapidly.

For second part of overall losses – losses in transformer core, the situation is opposite. When maximal value of magnetic induction increases, the value of core losses also increases (6).

$$P_{fe} = K_{fe} \cdot (\Delta B)^{\beta} \cdot A_C \cdot l_m \tag{6}$$

where

lm –Magnetic path length [cm]

β – Core loss exponent (for ferrite 2,6 - 2,7)

K_{fe}–parameter representing specific volume losses of material depending on saturation and switching frequency [W/cm3]

Losses in transformer´s core, in addition to value of saturation, depend on core geometry, which is defined by factor of area, length, and by material properties of magnetics (parameter Kfe). It was mentioned that the ideal design of transformer depends on optimal value of parameter ΔB, thus next formula must be valid: $P_{tot} = P_{Cu} + P_{fe} =$ minimum.

Graphical interpretation of this requirement is on fig.2. In order to minimize total transformer losses, next formulation must be valid:

$$\frac{dP_{tot}}{d(\Delta B)} = \frac{dP_{fe}}{d(\Delta B)} + \frac{dP_{Cu}}{d(\Delta B)} = 0 \tag{7}$$

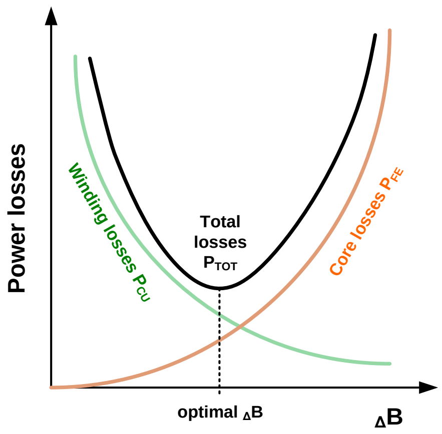

Fig. 2 Dependency of transformer losses on the ripple of magnetic induction

Because of non-uniform shape of Pcu and Pfe characteristics (fig. 2), it is not always true that optimal value of ΔB shall fulfill this condition: Pfe = Pcu. Therefore, the optimal value of ΔB must be found in order to meet:

$$\frac{dP_{fe}}{d(\Delta B)} = -\frac{dP_{cu}}{d(\Delta B)} \tag{8}$$

As can be seen from (5) and (6) it is clear, that transformer losses are instead of ΔB dependent on geometry and material properties of core. Targeting application requirements (high efficiency, high power density) transformer design must be focused almost on the proper selection of core properties. When selecting core material, it is suitable to focus on the operating frequency of converter and consequently select material with the highest value of ΔB for selected frequency (fig. 3).

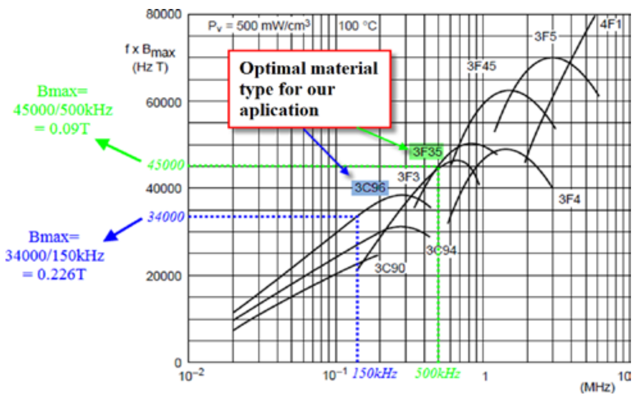

Fig. 3 Material selection curves for various operational conditions

Then, from material volume loss characteristics, it is possible to determine (fig. 4) expected core losses for selected operational point of transformer.

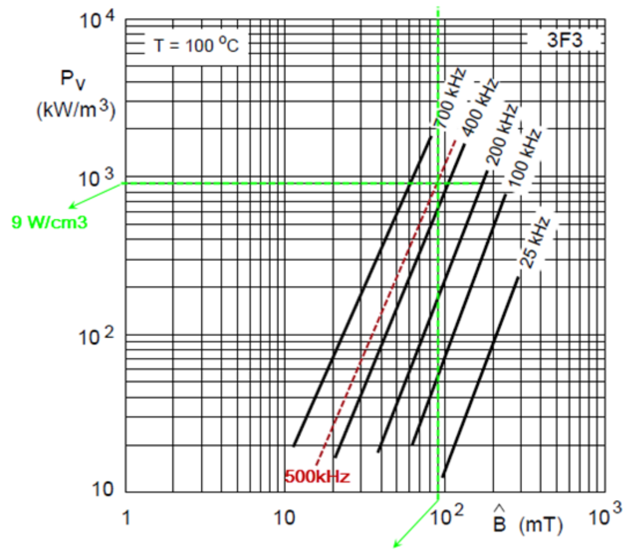

Fig. 4 Expected core losses for selected operation point

2.2 Transformer core selection for high efficiency, high power density operation

For the high efficiency and high power density applications of power converter it is known, that PQ or RM shape of transformer core is preferred. This is due to compact shape and due to possibility for bobbin-less winding design.

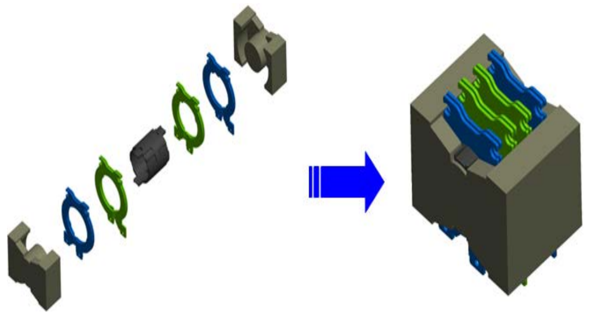

Fig. 5 Example of bobbin-less high-frequency transformer design

Design of high-frequency transformer is complex task when contradictory requirements must be taken into account. It is the core volume of transformer and its total loses. With the use of previous analysis (1) – (8) it is possible to evaluate transformer losses in dependency on saturation induction as well as on core volume (fig. 6). Through this process, it is possible to realize, what the amount of total transformer losses is. Thus optimal selection (not exceeding allowed transformer losses and the value of saturation induction) of the transformer core (shape/volume) can be done.

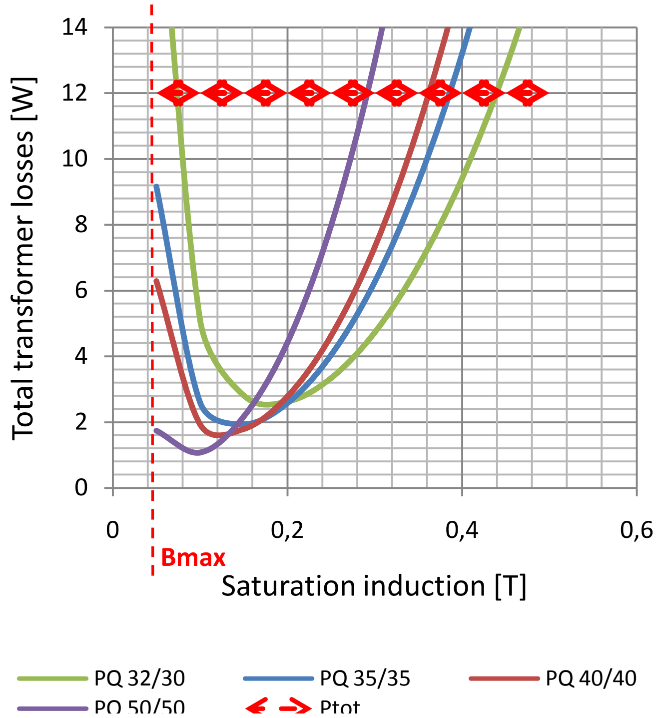

Fig. 6 Total transformer losses in dependency on the value of saturation induction and core volume

2.3 Application of optimal transformer design procedure on proposed LLC converter

Previous methodology of the optimal design of high frequency transformer was applied during design of proposed LLC converter. Its main electrical parameters are:

- switching frequency = 500 kHz,
- Output power = 500 W
- Input voltage = 400 V,
- Output voltage = 48 V
- K_{fe} = 5 W/cm3 ;
- K_U = 0,5; β = 2,6; ηtransf = 99,8%
- P_{tot} = 0,9 W

a) <u>Computation of U1 and Itot</u>

$$U_1 = D.T_{SW}.U_{INMAX} = 0{,}5.2e-6.400 = 400V/\mu s$$

$$I_{tot} = I_1 + \frac{1}{n} I_2 = \frac{10}{4} + \frac{1}{4} 10 = 5A$$

b) <u>Computation of K_g</u>

$$K_g \geq \frac{1{,}724e-6.(400e-6)^2.25.5^{(2/2{,}6)}}{4.0{,}5.(0{,}9)^{(4{,}6/2{,}6)}}.10^8 = 1{,}5e-3$$

, whereby based on the catalog data of ferrite cores, PQ 20/16 with Kg = 3,7e-3 may be a proper choice.

TABLE I
PQ20/16

properties	Values
Geometric constant Kg	3,7 e-3 cm^x
Cross-sectional area Sj	0,62 cm^2
Bobbin winding area So	0,256 cm^2
Mean lenght per turn MLT	4,4 cm
Magnetic path lenght lm	3,74 cm
Weight core	13g

c) Computation of ΔB

$$\Delta B == \left[10^8 \frac{1{,}724e-6.(400e-6)^2.25}{2.0{,}5} \cdot \frac{4{,}4}{0{,}256.(0{,}62)^3.3{,}74} \cdot \frac{1}{2{,}6.5}\right]^{(1/4{,}6)} = 230mT$$

What pose as high value compared to allowed saturation of core material 3F3 by Ferroxcube Bmax(500kHz) = 150 mT). Therefore selection of core with higher volume and higher specific volume losses is necessary. Selected core is the PQ26/20 with Kgfe = 7,2e-3.

TABLE II
PQ26/20

properties	Values
Geometric constant Kg	7,2 e-3 cm^x
Cross-sectional area Sj	1,19 cm^2
Bobbin winding area So	0,333 cm^2
Mean lenght per turn MLT	5,62cm
Magnetic path lenght lm	4,63cm
Weight core	31g

d) Recalculation of ΔB

$$\Delta B = \left[10^8 \frac{1{,}724e-6.(400e-6)^2.25}{2.0{,}5} \cdot \frac{5{,}62}{0{,}503.(1{,}18)^3.5{,}55} \cdot \frac{1}{2{,}6.5}\right]^{(1/4{,}6)} = 124mT$$

The final recalculation confirmed, that selected core PQ26/20 may be sufficiently designed for the use in proposed converter. The other suitable core geometries are EE30 and POT core 2616, whose influence on the efficiency will be investigated.

2.3 Ripple current cancelation by interleaved switching

The output current I_{out} of the LLC converter as is shown on the fig. 7 is given by the sum of the current i_{out} of rectifier diodes D_1 and D_2 and current of the filter capacitor i_{Cout}. It notes that a value of the output capacitor ripple current can lead to their destruction. Usage of the output choke in order to reduce the ripple of the output current is not perspective solution in the case of high density power supply, as a further choke is a bulky component, and introduces additional losses in the circuit.

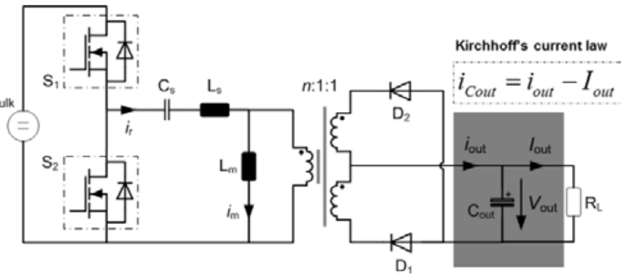

Fig. 7 Typical schematic of the LLC converter

By adapting 90 degrees' phase shift between switching of the LLC converter #1 and LLC converter #2, it is possible to achieve a significant decrease in the output capacitor's ripple current as is shown in Figure 8 [16].

This solution eliminates the need for output choke and allows to use output capacitors for significantly lower ripple current. Consequently, it is possible to optimize the number of output capacitors and thus increase the power density by reducing the volume of the converter.

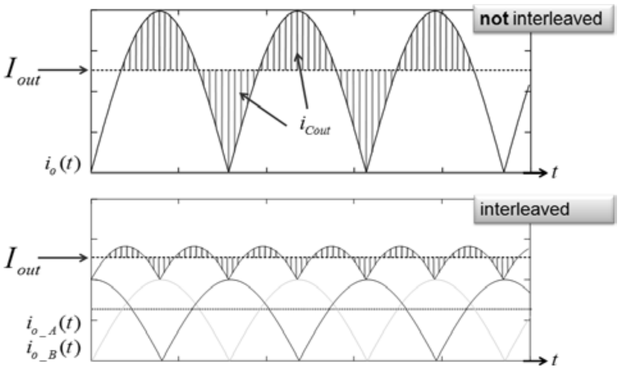

Fig. 8 Influence of interleaving for reduction of output capacitor's ripple current

In order to effectively reduce the ripple of the output current it is necessary for the two DC / DC converters to operate at the same switching frequency with the mutual phase shift of 90 °. Setting the different switching frequency of LLC #1 and LLC #2 in order to evenly share the output load is not the optimal solution. In addition, the change of the duty cycle in the case of converters with pulse-width modulation (PWM) control is a simple solution, but in the case of resonant converters this is not suitable.

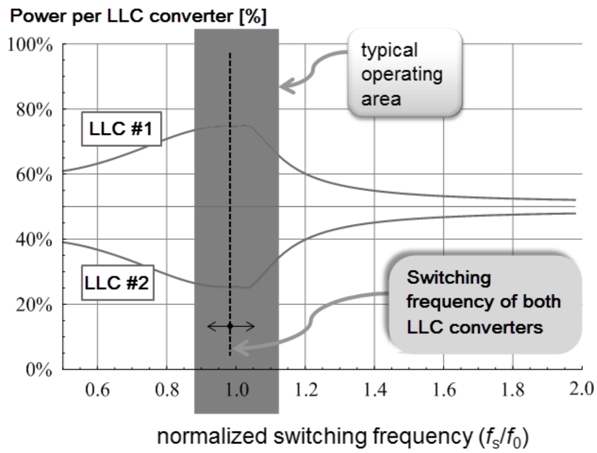

Fig. 9 Unbalanced distribution of output power between the LLC converter due to tolerances of the resonant components

The most suitable solution for ensuring the balanced output load sharing and reducing output ripple current of the parallel connected LLC converters can be achieved by split of input voltages of individual LLC converters (fig. 10).

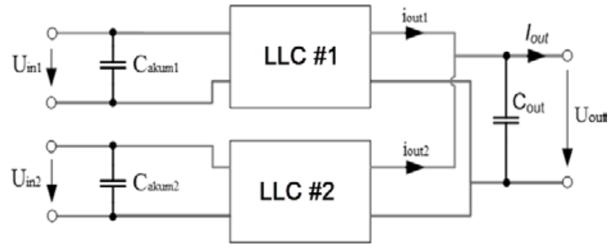

Fig. 10 Principle of the separated input voltage for parallel connected LLC converters

Figure 11 shows principle of the separated input voltages for parallel connected LLC converters. In order to achieve balanced load sharing between both LLC converters the input voltages Uin1 and Uin2 shall be adjusted according to the actual tolerance of the resonant components of the particular LLC converter.

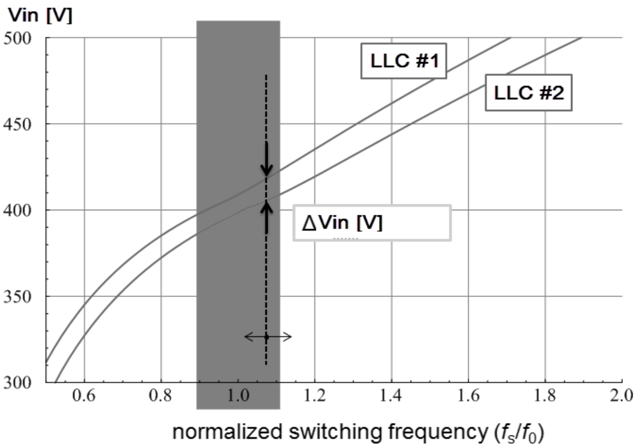

Fig. 11 Impact of the tolerance of resonant components on resonant frequency deviation

3 Interactive control system proposal

Purpose of the presented tool is on-line control of the high power density dual interleaved LLC converter. For that reason, the GUI for any kind of application with embedded DSP was designed. Digital control algorithm is running on the embedded DSP to control operation of LLC resonant converter. The control panel is running on the host computer (i.e. PC), which completes the entire solution by exposing and demonstrating parameters/capabilities of the DSP and target application (fig.12). This approach enables to interact with the target application and change the behavior of the power stage in real time. Beside that, all measured values can be displayed, what is done through the use of measuring cards. Utilizing of the described graphic user interface make it easy to demonstrate behavior of the LLC converter and can help to understand theory of operation for beginners or students.

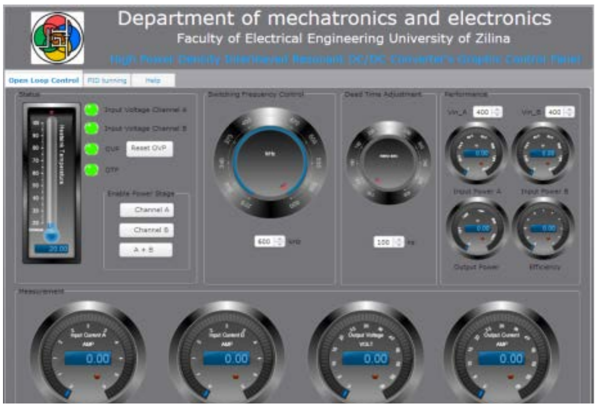

Fig. 12 Main window of the control panel.

4 Experimental verification

By entering the switching frequency in the control panel the user can move with the operational point of the LLC converter within whole operation range and consequently observe the change of waveforms online (fig. 13). Additionally with the change of the position of panel’s control items the user can control auxiliary functions of the hardware like over voltage protection, over current protection, under voltage of the DC bus, etc…(depends on the hardware implementation). Instead of that, proposed environment and control system enables to design PID controller and run converter in closed loop operation.

Embedding of the TI’s launchpad XL TMS320F2802x into design of the LLC converter is the easiest way how to implement the digital control capabilities to the design and enables designer to connect it to the computer by on-board JTAG emulator. Described Control Panel was designed with the use of GUI Composer Designer. The GUI Composer Designer is the design tool used for development of various industrial applications. GUI Composer is integrated into Code Composer Studio providing an integrated environment for development of target application and custom GUI within the same environment. GUI Composer apps can be designed and verified using full debug capabilities of Code Composer Studio.

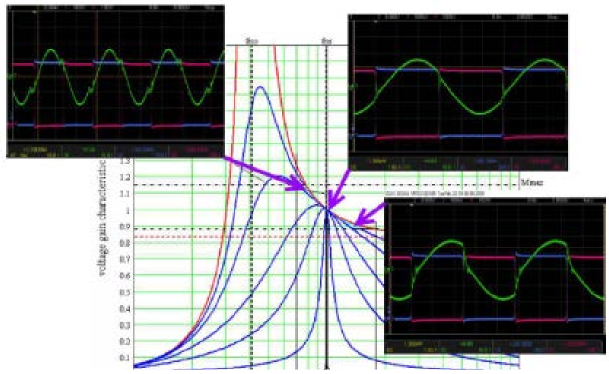

Fig. 13 Example of the interpretation of voltage gain characteristics and relevant operational waveforms of LLC converter during various conditions

The investigation of the operation was done on the experimental prototype (fig. 14) of dual interleaved LLC converter. The main input output parameters of this converter are:

- input voltage range: 200 – 400 Vdc
- output voltage range: 40 – 60 Vdc
- switching frequency: 200 – 600 kHz
- output power: 500 – 2500 W

This experimental prototype was interconnected with proposed control system and consequently regulation and control in real – time was verified. It might be seen (fig. 13) that interactive control enables to investigate whole regulation and operational range of the LLC converter, and also it is possible to investigate in detail each waveform of the main circuit. Among other things it is also possible to determine switching losses and overall efficiency of the converter during any operational condition (fig. 15).

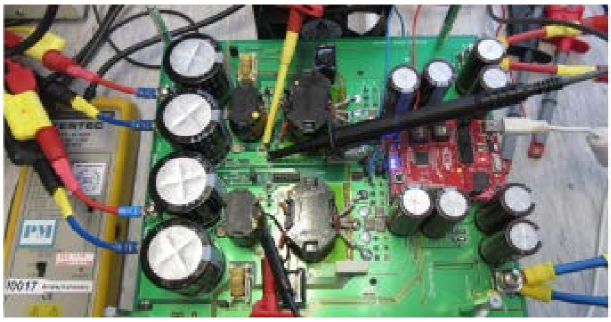

Fig. 14 Experimental prototype of high power density dual interleaved LLC resonant converter

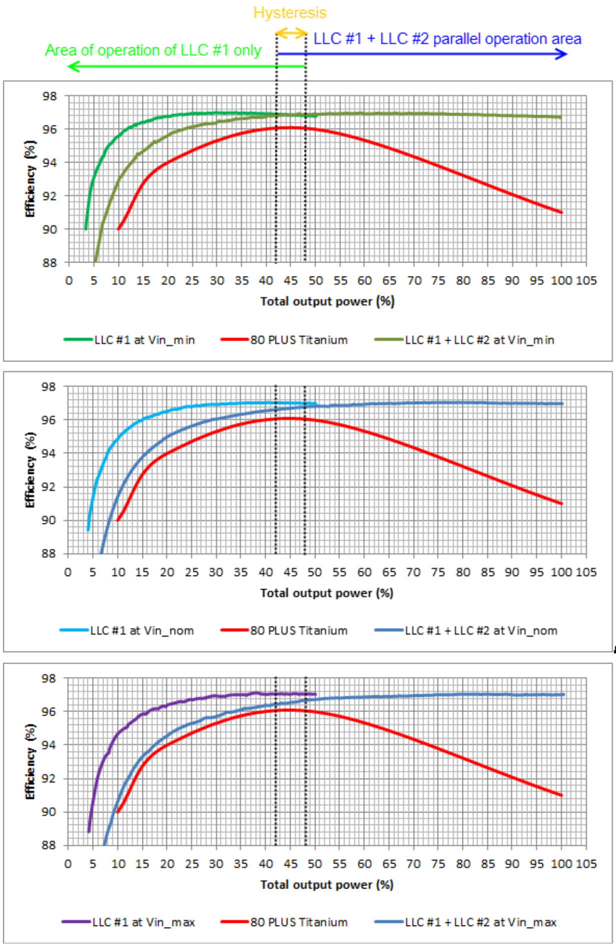

Fig. 15 Efficiency curves of dual interlevead LLC converter received with the use of interactive control and data management

4 Conclusion

In this paper, interleaved, parallel-operated LLC converter was described. Proposed converter´s design was focused on the achievement of improved qualitative indexes of power supplies for telecom-server applications. Based on the proper transformer design and based on the investigation of component´s tolerances, target operational parameters have been met. 500 kHz, 1,5kW LLC cells operated in parallel – interleaved mode extends almost constant high-efficiency operation from 45% of load up to the range of full – load of operation. The operation was verified with designed computer control system for proposed DC/DC converter. Principal behavior was analyzed using the control panel, running on host PC. For example operation modes below or above resonant frequency are investigated together with possibility of investigation within open or closed loop of control system. The system is suitable mainly for beginners or students, who are not familiar with operation of high frequency resonant converter.

Acknowledgement

The authors wish to thank Slovak grant agency APVV for the project no. 0396-15 - Research of perspective high-frequency converter systems with GaN technology.

References:

[1] Z. Hu, Y. Qiu, L. Wang and Y. F. Liu, "An Interleaved LLC Resonant Converter Operating at Constant Switching Frequency," in *IEEE Transactions on Power Electronics*, vol. 29, no. 6, pp. 2931-2943, June 2014.

[2] Shih-Ming Chen, Yong-Hong Haung, Yi-Yuan Chung, Yi-Hsun Hsieh and Tsorng-Juu Liang, "A novel interleaved LLC resonant converter," *Industrial Electronics Society, IECON 2013 - 39th Annual Conference of the IEEE*, Vienna, 2013, pp. 293-297.

[3] L. M. Wu and P. S. Chen, "Interleaved three-level LLC resonant converter with fixed-frequency PWM control," *2014 IEEE 36th International Telecommunications Energy Conference (INTELEC)*, Vancouver, BC, 2014, pp. 1-8.

[4] Kindl, V.; Kavalir, T.; Pechanek, R.; Skala, B.;Sobra, J., "Key construction aspects of resonant wireless low power transfer system," ELEKTRO, 2014 , vol., no., pp.303,306, 19-20 May 2014

[5] Brandstetter, P.; Chlebis, P.; Simonik, P.: Active Power Filter with Soft Switching, In: INTERNATIONAL REVIEW OF ELECTRICAL ENGINEERING-IREE Vol: 5, Iss: 6 Pages: 2516-2526

[6] Kovacova, I., Kovac, D.: Inductive coupling of power converter´s EMC, In: Acta polytechnica hungarica, Vol:6, Issue:2, pp. 41-53, 2009.
[7] Dobrucky, B., Laskody, T., Prazenica, M., Kascak, S.: Analysis of VSI and MxC Converters Fed Two-Phase Induction Motor with the Same Magnitude of Fundamental Harmonic Voltages, In: International Review of Electrical Engineering - IREE, Vol. 9, No. 5 2014, pp. 989-902, ISSN 1827-6660,
[8] W. Dai, "Modeling and efficiency-based control of interleaved LLC converters for PV DC microgrid," *Industry Applications Society Annual Meeting, 2015 IEEE*, Addison, TX, 2015, pp. 1-8.
[9] B. Yang: “Topology investigation for front end dc/dc power conversion for distributed power system”, Dissertation Virginia Polytechnic Institute and State University, 2003.
[10] B. Yang, F. C. Lee, A. J. Zhang and G. Huang: “LLC resonant converter for front end dc/dc conversion”, IEEE APEC 2002, Vol.2, pp. 1108 – 1112.
[11] Nayak, D.K. & Reddy, S.R. Arab J: Comparison of the synchronous-rectified Push-Pull converter with LLC DC to DC Converter, In Sci Eng (2013) 38: 913. doi:10.1007/s13369-012-0365-4
[12] Böhm, R., Rehtanz, C. & Franke, J.: Inverter-based hybrid compensation systems contributing to grid stabilization in medium voltage distribution networks with decentralized, renewable generation, In Electr. Eng. (2016) 98: 355. doi:10.1007/s00202-016-0425-y
[13] T. Jin and K.. Smedley: “Multiphase LLC series resonant converter for microprocessor voltage regulation”, IEEE 41st Industry Applications Conference – IAS, Vol. 5, 8-12 Oct. 2006, pp. 2136 – 2143.
[14] I. Apeland and R. Myhre: “Phase-shifted resonant converter having reduced output ripple”, US patent 6970366 B2, Nov. 2005.
[15] H. Figge, T. Grote, N. Froehleke. J. Boecker and P. Ide: “Paralleling of LLC resonant converter using frequency controlled current balancing”, IEEE PESC 2008, June 2008 pp. 1080 – 1085.
[16] Wenming GONG, Shuju Hu, Martin SHAN, Honghua XU, “ Robus currnet control design of a three phase voltage source converter” , MPCE J. Mod. Power Syst. Clean Energy (2014) 2(1):16–22 DOI 10.1007/s40565-014-0051-5
[17] Xiaoqianf GUO, Huaibao WANG, Zhigang LU, Baocheng WANG, “New inverter topology for ground current suppression in transformerless photovoltaic system application” MPCE J. Mod. Power Syst. Clean Energy (2014) 2(2):191–194 DOI 10.1007/s40565-014-0057-z
[18] Mingfei Wu, Dylan Dah-Chuan LU, “Active stabilization methods of electric power systems with constant power loads: a review” MPCE J. Mod. Power Syst. Clean Energy (2014) 2(3):233–243 DOI 10.1007/s40565-014-0066-y
[19] J. Dudrik, P. Spanik, N. D. Trip: "Zero-Voltage and Zero-Current Switching Full-Bridge; DC Converter With Auxiliary Transformer",

Power Electronics, IEEE Transactions, Vol. 21, issue 5, ISSN 0885- 8993,p. 1328 - 1335, 06 september 2006
[20] Dobrucký, B., Špánik, P., Kabašta, M.: Power Electronic Two – phase Ortogonal System with HF Input and Variable Ouput, In: Electronics and Electrical Engineering No. 1 (89) Kaunas 2009, pp. 9 -14, ISSN 1392 - 1215
[21] Pavlanin, R., Spanik, p., Dobrucky, B.: Comparison of Multi-Resonant- and Hysteresis Band Controllers used in Current Control Loop of Shunt Active Power Filter, In: Renewable Energy & Power Quality Journal, No. 10, 25. 4. 2012, pp. 846, ISSN 2172-038X,
[22] Kindl, V.; Kavalir, T.; Pechanek, R.; Skala, B.; Sobra, J., "Key construction aspects of resonant wireless low power transfer system," ELEKTRO, 2014 , vol., no., pp.303,306, 19-20 May 2014
[23] Koscelnik, J., Sedo, J., Dobrucky, B.: Modeling of Resonant Converter with Nonlinear Inductance, In: 2014 INTERNATIONAL CONFERENCE ON APPLIED ELECTRONICS (AE), pp 153-156, ISBN:978-80-261-0276-2
[24] Brandstetter, P., Chlebis, P., Palacky, P.: Application of RBF network in rotor time constant adaptation, In: Elektronika IR elektrotechnika, Issue:7, pp.21-26, 2011.
[25] Brandstetter P., Chlebis P., Simonik P.: "Control Algorithms of Active Power Filters", Progress In Electromagnetics Research Symposium Proceedings, Cambridge, USA, 2010.
[26] Brandstetter, P.; Chlebis, P.; Simonik, P.: Active Power Filter with Soft Switching, In: INTERNATIONAL REVIEW OF

ELECTRICAL ENGINEERING-IREE Vol: 5, Iss: 6 Pages: 2516-2526

[27] Ferkova, Z., Franka, M., Kuchta, J.: Electromagnetic design of Ironless Permanent Magnet Synchronous Linear motor, In: International symposium on power electronics, electrical drives, automation and motion (SPEEDAM), Italy, June 11-13, 2008, pp. 721-726.

[28] Kovacova, I., Kovac, D.: Inductive coupling of power converter´s EMC, In: Acta polytechnica hungarica, Vol:6, Issue:2, pp. 41-53, 2009.

[29] Dobrucky, B., Laskody, T., Prazenica, M.: A Novel Supply System for Two- Phase Induction Motor by Single Leg Matrix Converter, In: Elektronika ir Elektrotechnika, Vol. 21, No. 4, 2015, pp. 13-16, ISSN 1392-1215

[30] Zaskalicky, P., Dobrucky, B., Prazenica, M.: Analysis and Modeling of Converter with PWM Output for Two-Phase Applications, In: Electronics and Electrical Engineering, Vol. 20, No. 1 (2014), Kaunas 2014, pp. 25-28, ISSN 1392–1215

[31] Dobrucky, B, Prazenica, M, Kascak, S, Kassa, J: HF Link LCTLC Resonant Converter with LF AC Output, In: 38th Annual Conference on IEEE-Industrial-Electronics-Society (IECON), CANADA 2012, pp. 447-452, ISBN:978-1-4673-2421-2, ISSN: 1553-572X,

[32] HARGAS, L., KONIAR. D., LONCOVA, Z., HRIANKA, M., Hurtukova, Z., SIMONOVA, A.: Regular Shapes Detection for Analysis of Biomedical Image Seuences, In: 20th International Conference on Applied Electronics, APPEL 2015, IEEE, Pilsen 2015, pp. 49-52, ISBN 978-80-261-0385-1, ISSN 1803-7232

[33] LONCOVA, Z., HARGAS, L., KONIAR, D., HRIANKA, M., SIMONOVA, A.: Parameters measurement of the object in a video sequence, In: 13th International IFAC Conference on Programmable Devices and Embedded Sysytems : Cracow, Poland, 13-15 May 2015, - ISSN 2405-8963

[34] Koniar, D., Hargas, L., Stofan, S., Hrianka, M.: High Speed Video System for Tissue Measurement Based on PWM Regulated Dimming and Virtual Instrumentation, ELEKTRONIKA IR ELEKTROTECHNIKA, Issue 10, Pages 169-172, 2010

[35] Nayak, D.K. & Reddy, S.R. Arab J: Comparison of the synchronous-rectified Push-Pull

[36] converter with LLC DC to DC Converter, In Sci Eng (2013) 38: 913. doi:10.1007/s13369-012-0365-4

[37] Böhm, R., Rehtanz, C. & Franke, J.: Inverter-based hybrid compensation systems contributing to grid stabilization in medium voltage distribution networks with decentralized, renewable generation, In Electr. Eng. (2016) 98: 355. doi:10.1007/s00202-016-0425-y

[38] Acharjee, P. & Goswami,: Power flow analysis undre critical conditions by the linear perturbation- based simple algorithm, In S.K. Electr Eng (2012) 94: 187. doi:10.1007/s00202-011-0228-0

[39] de Miranda, C.M. & Pichorim,: Self-resonant frequencies of air-core singe-layer soleniod coils calculated by a simple method S.F. Electr Eng (2015) 97: 57. doi:10.1007/s00202-014-0312-3

[40] Petrović, : Current-tunable current-mode RMS detector, In P.B. Electr Eng (2015) 97: 65. doi:10.1007/s00202-014-0313-2

[41] Meral, M.E., Cuma, M.U., Teke, A. : Experimental and simulation based study of an adaptive filter controlled solid state transfer switch, In Electr Eng (2014) 96: 385. doi:10.1007/s00202-014-0305-2